Chapter 2

Theoretical fundamentals. Propagation equations

In this chapter we establish the theoretical basis for the further analytical and numerical studies.

2.1 The propagation equation

The standard theoretical method in nonlinear and fiber optics is the slowly-varying envelope approximation. In many cases, the time dependence of the electric field consists of an envelope which varies on the time scale of the pulse duration modulated by oscillations on the time scale of the reverse frequency. Therefore, the rapidly varying part (carrier) of the electric field $\vec{E}(\vec{r},t)$ can be separated from the slowly varying envelope $\vec{A}(\vec{r},t)$:

$$\vec{E}(\vec{r},t) = \frac{1}{2}\vec{A}(\vec{r},t)\exp[i\omega_0 t - k(\omega_0)z] + c.c.\ , \tag{2.1}$$

where $\vec{r} = \{x, y, z\}$, ω_0 is the input carrier frequency, $k(\omega) = n(\omega)\omega/c$ the wavevector and $n(\omega)$ the frequency-dependant refractive index. In the SVEA the slowly varying envelope is assumed to satisfy the condition

$$\left|\frac{\partial \vec{A}}{\partial t}\right| \ll \omega_0 \left|\vec{A}\right| \ , \tag{2.2}$$

which is fulfilled if and only if the spectral width of a pulse $\Delta\omega$ is much smaller than the carrier frequency ω_0 of the pulse: $\Delta\omega \ll \omega_0$. The latter condition allows to neglect higher-order terms in the Taylor expansion of $k(\omega)$ around ω_0 when determining the influence of dispersive effects:

$$k(\omega) = k(\omega_0) + k'(\omega_o)(\omega - \omega_0) + \frac{k''(\omega_0)}{2}(\omega - \omega_0)^2 + \frac{k'''(\omega_0)}{6}(\omega - \omega_0)^3 + \dots \tag{2.3}$$

Obviously, these approximations are no longer valid for radiation with ultra-wide spectra such as pulses with a duration approaching one optical cycle.

Pulse propagation without the special prerequisites of the SVEA can be studied by the numerical solution of Maxwell's equations by the finite-difference time-domain method (see Ref. [39, 40, 14] and references therein). In this method, two shifted space-time grids in the scale of the wavelength/optical period are used for the description of the electric and magnetic fields of the pulse. The values of the field for the next time step are found by a special "leap-frog" algorithm which ensures the second-order accuracy of this method. However, due to the high-resolution grid needed in *both* space and time the large numerical effort in this approach limits the possible propagation lengths to a few mm. In several papers various improved equations have been derived that allow the theoretical description beyond the validity of the standard approximations [41, 42, 43]. In the following we give a systematic derivation of a first-order unidirectional propagation equation without

the use of the SVEA and the Taylor expansion of the linear refraction index. This equation extends previously derived equations into the non-paraxial and extremely nonlinear region from which the basic equations of Ref. [43] or [41] can be derived in a physically transparent manner.

We start from the Maxwell equations in the form

$$\nabla \times \vec{E} = \frac{\partial \vec{B}}{\partial t}, \quad \nabla \times \vec{H} = \frac{\partial \vec{D}}{\partial t} + \vec{J}_f,$$
$$\nabla \cdot \vec{D} = \rho_f, \quad \nabla \cdot \vec{B} = 0. \tag{2.4}$$

Here $\vec{H}$ is the magnetic field, $\vec{J}_f$ and ρ_f are the current density and the charge density, $\vec{B}$ and $\vec{D}$ are given by the constitutive relations $\vec{D} = \epsilon_0 \vec{E} + \vec{P}$, $\vec{B} = \mu_0 \vec{H} + \vec{M}$ where ϵ_0 and μ_0 are vacuum permittivity and permeability, respectively, and $\vec{P}$ and $\vec{M}$ are induced electric and magnetic polarizations. The curl $\nabla\times$ is applied to the first equation of this set, and we can get the propagation of pulses in nonlinear media in the form

$$\left(\frac{\partial^2}{\partial z^2} + \Delta_\perp \right) \vec{E} - \frac{1}{c^2} \frac{\partial^2}{\partial t^2} \vec{E} = \mu_0 \frac{\partial^2}{\partial t^2} \vec{P} \,, \tag{2.5}$$

where

$$\Delta_\perp = \partial^2/\partial x^2 + \partial^2/\partial y^2. \tag{2.6}$$

Assumptions necessary for rewriting (2.4) in the form (2.5) are

- the density of free charges and currents is zero
- the medium is non-magnetic
- dielectric permittivity is piecewise constant and scalar

which are satisfied with a high accuracy for propagation in fibers. The latter assumption means that a fiber can be separated into several regions so

that within each of them the dielectric permittivity is a constant. On the boundaries of these regions, the usual boundary conditions are set, i.e. the continuity of a tangential component of $\vec{E}$ and a normal component of $\vec{D}$. Substituting the Fourier-transformed field

$$\vec{E}(z,\omega,\vec{k}_\perp) = \int_{-\infty}^{\infty} \exp(i\omega t - i\vec{k}_\perp \vec{r_\perp})\vec{E}(\vec{r},t)dtd\vec{r}_\perp, \tag{2.7}$$

where $\vec{r}_\perp = \{x,y\}$, $\vec{k}_\perp = \{k_x,k_y\}$ into the wave equation (2.5) we obtain

$$\frac{\partial^2 \vec{E}(z,\omega,\vec{k}_\perp)}{\partial z^2} \quad + \quad \beta_{\mathrm{NL}}^2(\omega)\vec{E}(z,\omega,\vec{k}_\perp) = 0 \tag{2.8}$$

with

$$\beta_{\mathrm{NL}}(\omega,\vec{k}_\perp) = \left\{ \frac{\omega^2}{c^2}[1+\chi(\omega)] - \vec{k}_\perp^2 + \mu_0\omega^2 B_{\mathrm{NL}}(z,\omega,\vec{k}_\perp) \right\}^{1/2}. \tag{2.9}$$

We assume $\vec{P_{\mathrm{NL}}}||\vec{E}$, which requires that the

- medium be isotropic,

to get

$$B_{\mathrm{NL}} = \frac{P_{\mathrm{NL}}(z,\omega,\vec{k}_\perp)}{E(z,\omega,\vec{k}_\perp)}\,. \tag{2.10}$$

Here we separate the polarization into a linear and a nonlinear part as

$$\vec{P} = \vec{P}_L(\vec{r},\omega) + \vec{P}_{\mathrm{NL}}(\vec{r},\omega), \tag{2.11}$$

where $\vec{P}_{\mathrm{NL}}(\vec{r},\omega)$ is the Fourier transform of the nonlinear part of the polarization and

$$\vec{P}_L(\vec{r},\omega) = \epsilon_0[n^2(\omega)-1]\vec{E}(\vec{r},\omega) \tag{2.12}$$

its linear part.

In most typical situations the condition $\mu_0\omega^2 B_{\mathrm{NL}} \ll 2\beta_{\mathrm{NL}}^2$ is satisfied with high accuracy, because the contribution of nonlinear polarization is

much smaller than the field itself for any practical situation in which we can neglect contribution from ionization as we do here. Therefore, the separation

$$\partial^2/\partial z^2 + \beta_{\mathrm{NL}}^2(\omega) = [\partial/\partial z - i\beta_{\mathrm{NL}}(\omega)][\partial/\partial z + i\beta_{\mathrm{NL}}(\omega)] \tag{2.13}$$

is possible. The electric field can be separated into a forward E^+ and a backward E^- propagating part:

$$\vec{E}(z, \vec{k}_\perp, \omega) = \vec{E}^+(z, \vec{k}_\perp, \omega) + \vec{E}^-(z, \vec{k}_\perp, \omega). \tag{2.14}$$

Let us consider a pulse propagating in the forward direction along the z-axis $\vec{E}^+(z, \vec{k}_\perp, \omega) \sim \exp[ik(\omega)z]\vec{E}_0(z, \vec{k}_\perp, \omega)$ and neglect waves propagating backward. This requires that the refractive index be constant or a smooth, slowly changing function of the z coordinate. Therefore we have

$$\frac{\partial \vec{E}^+}{\partial z}(z, \vec{k}_\perp, \omega) = i\beta_{\mathrm{NL}}(z, \vec{k}_\perp, \omega)\vec{E}^+(z, \vec{k}_\perp, \omega)\ , \tag{2.15}$$

when the effect of the backward wave on B_{NL} can be neglected. This equation is applicable for the description of light propagation, if the following conditions are satisfied:

- The product of the nonlinear refractive index and intensity is much less than unity. This is valid for both materials considered here (fused silica and argon) as well as for almost all other materials for the intensities below the damage threshold;

- The nonlinear polarization and the electric field have the same direction;

- The initial condition consists only of the wave propagating in one direction. This requirement is always satisfied after certain propagation

length, even if the input field contained both forward and backward waves initially. Each of the waves can be described by Eq.(2.15);

- The dependence of the refractive index on the propagation length, if present, must be weak.

For the backward wave we find

$$\frac{\partial \vec{E}^-}{\partial z}(z, \vec{k}_\perp, \omega) = -i\beta_{\mathrm{NL}}(z, \vec{k}_\perp, \omega)\vec{E}^-(z, \vec{k}_\perp, \omega)\ . \tag{2.16}$$

Equation (2.15) represents a more general approach than the standard one and is even more accurate than previously derived evolution equations without SVEA as presented in [43]. This equation includes in the theoretical analysis broad bandwidth, sharp temporal features, space-time coupling and higher-order nonlinear dispersive effects. Note that the SVEA with paraxial approximation for the transverse momentum fails to describe self-focusing in dispersive media accurately long before the temporal structure reaches the time of an optical cycle [44]. This effect is a result of space-time focusing of short pulses leading to a reduced axially projected group velocity of wide-angle rays in the angular spectra. Equation (2.15) can be numerically solved by the second-order split-step Fourier method.

The square root in Eq. (2.9) is expanded as

$$\beta(\omega, \vec{k}_\perp) \simeq k(\omega) - \frac{k_\perp^2}{2k(\omega)} + \frac{\mu_0\omega^2}{2k(\omega)}B_{\mathrm{NL}} \tag{2.17}$$

which additionally requires

- paraxial propagation.

However, space-time coupling is still taken into account. To account for

losses, $k(\omega)$ can be made complex: $k(\omega) = k_0(\omega) + i\alpha(\omega)$. With the introduction of the moving time coordinates $\xi = z, \eta = t - zn_g/c$ with

$$\partial/\partial z = \partial/\partial\xi - n_g c^{-1}\partial/\partial\eta \tag{2.18}$$

we obtain the following basic equation in Fourier presentation which we denote in the following as forward Maxwell equation (FME) [43]:

$$\begin{aligned}\frac{\partial\vec{E}(\vec{r},\omega)}{\partial\xi} &= i\left[k(\omega) - \frac{\omega n_g}{c}\right]\vec{E}(\vec{r},\omega) \\ &+ \frac{i}{2k(\omega)}\Delta_\perp\vec{E}(\vec{r},\omega) + \frac{i\mu_0\omega c}{2n(\omega)}\vec{P}_{\mathrm{NL}}(\vec{r},\omega).\end{aligned} \tag{2.19}$$

Here n_g is a group refractive index $n_g = n(\omega) + \omega(dn/d\omega)$ calculated at any frequency inside the spectrum. The choice of n_g determines only an arbitrary time shift. Equation (2.19) is a generalization of the so-called *reduced* Maxwell equation [41, 49] which is valid only for a

- refractive index close to unity
- and also with neglection of the back propagating wave.

This equation is obtained from (2.5) by the substitution $n(\omega) - 1 \simeq [n^2(\omega) - 1]/2$ and back transformation into the time domain:

$$\frac{\partial\vec{E}}{\partial\xi} = -\frac{1}{2\epsilon_0 c}\frac{\partial\vec{P}}{\partial\eta}\ . \tag{2.20}$$

This equation is a useful tool for examining the nonlinear effects of ultrabroadband radiation in gaseous media. It was recently applied for the study of pulse compression and SC generation by the optical Kerr effect [14, 45] or by high-order stimulated Raman scattering [46, 47] in hollow waveguides. In Ref. [48] an extended version of this equation was used with inclusion of the

diffraction term. However, as one would expect, for optically dense media ($n-1 \sim 1$) solutions of this equation differ from those of the exact Maxwell equation as can be seen by comparison of FME and the reduced Maxwell equation in Fig. 2.1(b). It can be seen that results obtained by using FME are in good agreement with exact results obtained by the FDTD method in Ref. [14]. This shows that Eq. (2.19) is completely valid for description of ultrabroadband radiation with good accuracy and reasonable numerical effort.

Equation (2.19) generalizes the standard approximate evolution equation for the envelope in nonlinear optics. To show this, we introduce the envelope $A(\vec{\xi},\eta)$ as given by Eq. (2.1), choose the same prerequisites (2.2) and expand $\beta(\omega)$ in the form (2.17) around ω_0. After substitution of (2.1) into (2.19) the propagation equation for the linearly polarized field of a plane wave takes the form which can be found elsewhere [50]

$$\frac{\partial \vec{A}}{\partial \xi} + \frac{i}{2}\beta'' \frac{\partial^2 \vec{A}}{\partial \eta^2} - \frac{1}{6}\beta''' \frac{\partial \vec{A}}{\partial \eta^3} = i\gamma' \left(|A^2|\vec{A} + \frac{i}{\omega_0}\frac{\partial |A|^2 \vec{A}}{\partial \eta} \right) - \alpha A \,, \qquad (2.21)$$

where α is loss and $\gamma' = n_2 n \omega \epsilon_0 / 2$ is the nonlinear coefficient. This equation can be further simplified if

- higher-order nonlinear and dispersive effects as well as loss can be neglected, which requires still narrower spectrum.

In this case Eq.(2.21) reduces to the nonlinear Schrödinger equation (NSE) in the form

$$\frac{\partial \vec{A}}{\partial z} + \frac{i}{2}\beta'' \frac{\partial^2 \vec{A}}{\partial \eta^2} = i\gamma' \left(|A^2|\vec{A} \right) \,. \qquad (2.22)$$

This equation can be solved analytically by the inverse scattering problem method.

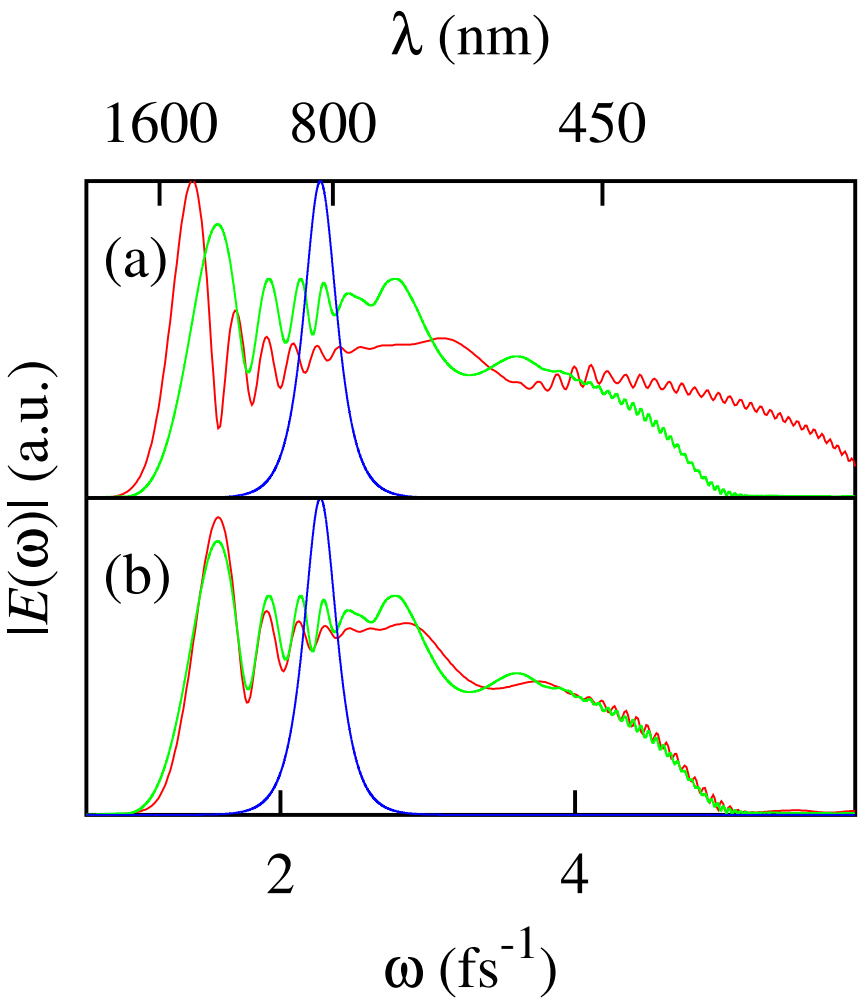

Figure 2.1: Pulse spectra calculated by different propagation equations. Spectra of a 40-TW/cm^2, 15-fs sech-shaped pulse after propagating 0.5 mm of a standard fiber calculated by the full Maxwell equation, obtained in [14] are shown by the green curves in (a) and (b). For comparison, by red curves are shown the solutions of FME (b) and reduced Maxwell equations (a). In contrast to reduced Maxwell equation, FME shows good agreement with exact calculation. The initial spectrum (scaled) is shown by the blue curves.

The same procedure can be applied if the nonlinear interaction of waves with different carrier frequencies is considered, for example, in a degenerate four-wave mixing (FWM). Pump, signal and idler pulses with central frequencies $\omega_P, \omega_S, \omega_I = 2\omega_P - \omega_S$ interact through the Kerr nonlinearity $\vec{P}_{\mathrm{K}}$. In this case using SVEA the linearly polarized electric field is presented by

$$E(z,t) = 1/2 \sum_j A_j(z,t) \exp[i(k_j z - \omega_j t)] + \text{c.c.} \tag{2.23}$$

($j = S, P, I$) and from Eq. (2.19) three propagation equations follow for A_P,A_S, and A_I describing the process of FWM:

$$\begin{aligned}
&\frac{\partial A_{\mathrm{P}}}{\partial z} = A_{\mathrm{P}} \left(-\alpha + i\gamma'_{\mathrm{P}}[|A_{\mathrm{P}}|^2 + 2|A_{\mathrm{I}}|^2 + 2|A_{\mathrm{S}}|^2]\right) \\
+ \quad & 2i\frac{\omega_P n_2}{c} A^*_{\mathrm{P}} A_{\mathrm{S}} A_{\mathrm{I}} \exp(i\Delta_k z) + i\beta_2(\omega_P)\frac{\partial^2 A_{\mathrm{P}}}{\partial \eta^2} \\
&\frac{\partial A_{\mathrm{S}}}{\partial z} = A_{\mathrm{S}} \left(-\alpha + i\gamma'_{\mathrm{S}}[|A_{\mathrm{S}}|^2 + 2|A_{\mathrm{P}}|^2 + 2|A_{\mathrm{I}}|^2]\right) \\
+ \quad & i\frac{\omega_S n_2}{c} A^*_{\mathrm{I}} A^2_{\mathrm{P}} \exp(-i\Delta_k z) + \left(\frac{1}{v_{g,\mathrm{P}}} - \frac{1}{v_{g,\mathrm{S}}}\right)\frac{\partial A_{\mathrm{S}}}{\partial \eta} + i\beta_2(\omega_S)\frac{\partial^2 A_{\mathrm{S}}}{\partial \eta^2} \\
&\frac{\partial A_{\mathrm{I}}}{\partial z} = A_{\mathrm{I}} \left(-\alpha + i\gamma'_{\mathrm{I}}[|A_{\mathrm{I}}|^2 + 2|A_{\mathrm{S}}|^2 + 2|A_{\mathrm{P}}|^2]\right) \\
+ \quad & i\frac{\omega_I n_2}{c} A^*_{\mathrm{S}} A^2_{\mathrm{P}} \exp(-i\Delta_k z) + \left(\frac{1}{v_{g,\mathrm{P}}} - \frac{1}{v_{g,\mathrm{I}}}\right)\frac{\partial A_{\mathrm{I}}}{\partial \eta} \\
+ \quad & i\beta_2(\omega_I)\frac{\partial^2 A_{\mathrm{I}}}{\partial \eta^2}.
\end{aligned} \tag{2.24}$$

Here $v_{g,j} = c/n_{g,j}$ are the group velocities of the corresponding waves, $\Delta k_0 = \beta(\omega_S) + \beta(\omega_I) - 2\beta(\omega_P)$ is the wavevector mismatch. The additional advantage of the evolution equation (2.19) is that all spectral components that can take part in a given process are included automatically in a single equation. This is particularly favorable if different processes can affect the propagation. The cost for this more general approach with a single evolution equation is the necessarily higher resolution of the temporal grid. The temporal grid

step dt should be much less than the period of radiation, while in the SVEA the resolution is in the scale of the envelope. However, in contrast to FDTD methods, the numerical step dz in *space* does not need to be much shorter than the wavelength, and in fact can be several mm. This explains the advantage of FME over FDTD methods, where dz cannot be made larger than cdt.

The differencies between the different propagation equations, including the propagation equation in fibers which will be derived later, are summarized in the Table 2.1.

Propagation equation	Prerequisites	Advantages	Disadvantages
Wave equation (2.5)	ϵ is piecewise constant	Most general	Requires a tremendous numerical effort
Forward Maxwell equation (2.19)	$dn/dz \ll \lambda$, forward propagation	Can be effectively solved numerically	
FME in fibers (2.66)	Weak selffocusing	1+1-dimensional	Limits maximum power
Reduced Maxwell equation (2.20)	$n(\omega) - 1 \ll 1$	None in comparison with FME	Not valid for optically dense ($n - 1 \sim 1$) media
Generalized nonlinear Schrödinger equation (2.21)	Narrow spectrum, SVEA	Usual equation with SVEA	Not applicable for broad spectra
Nonlinear Schrödinger equation (2.22)	Still narrower spectrum	Can be solved analytically	Does not include higher-order effects

Table 2.1: The comparison of different propagation equations. Note that requirements for more general equations apply also for less general, e.g. reduced Maxwell equation is valid only when the prerequisites of the wave equation are fulfilled.

2.1.1 Dispersion and nonlinear polarization

Up to this point, the specific form of the polarization $\vec{P}$ as a function of $\vec{E}$ as well as the physical considerations determining it, have not been specified. We start from the consideration of the linear polarization. Under the influence of the electric field, the dipole momentum is induced in the medium due to the redistribution of charged particles. The general form for the linear term in the expression for the polarization can be written as

$$\vec{P}_L(t) = \epsilon_0 \int_0^\infty \hat{\chi}(\tau)\vec{E}(t-\tau)d\tau. \tag{2.25}$$

Here we neglect effects of optical activity as well as other non-local effects (dependence of the polarization on the electric field in adjacent points). The quantity $\hat{\chi}(\tau)$ represents a delayed response of a medium to the electric field. Generally it is a tensor, but since optical fibers are homogeneous, it reduces to a scalar in our case. The previous convolution expression can be reformulated more conveniently in the frequency domain:

$$\vec{P_L}(\omega) = \epsilon_0 \chi(\omega) E(\omega). \tag{2.26}$$

For the linear propagation problems, the susceptibility χ is related to the refractive index n by $n^2 - 1 = \chi$. It can be real or complex, with the imaginary part describing the losses.

The physical origin of the delayed response of the medium can be understood by means of a classical model of electrons moving under an action of an external field. The binding forces of atoms are described as a potential $\omega_j^2 x_j^2/2$, where ω_j characterises the j'th group of the electrons which consist of f_j particles per unit volume and $\vec{x_j}$ is the displacement for the j'th group.

The polarization is given by (see, for example, [51])

$$\vec{P} = -e \sum_j f_j \vec{x_j}. \tag{2.27}$$

The equation of electron motion is written as

$$\frac{d^2\vec{x_j}}{dt^2} + g_j \frac{d\vec{x_j}}{dt} + \omega_j^2 \vec{x_j} = -\frac{\vec{E}e}{m}, \tag{2.28}$$

Here e and m are the electron charge and mass, respectively, and the effects of the magnetic field are neglected. The effects of loss are also introduced through g_j. The solution for the harmonic driving field $E_0 \exp(-i\omega_0 t)$ can be easily found, which yields

$$\vec{x_j} = -\frac{e\vec{E}}{m[\omega_j^2 - \omega_0^2 - ig_j\omega_0]} \tag{2.29}$$

and substituting into (2.27) results in

$$\chi(\omega) = \frac{e^2}{m\epsilon_0} \sum_j \frac{f_j}{\omega_j^2 - \omega_0^2 - ig_j\omega_0}. \tag{2.30}$$

Thus the susceptibility is determined as a sum of the contributions from several absorption lines. The dampings g_j determine the widths, and frequencies ω_j the positions of these lines, respectively. For dense media, the effect of the induced polarization on the driving field should be taken into account, which can be done by replacing $\vec{E}$ in the driving field by $\vec{E} + \vec{P}/(3\epsilon_0)$ (so-called Lorentz-Lorentz model). The exact quantum model yields an expression identical to (2.30), but with the values of f_j, ω_j and g_j calculated from the wavefunctions of the electronic states. The frequencies ω_j are replaced by the energy level distances $(E_1 - E_2)/\hbar$, and the square of the corresponding dipole moments appear in f_j. Nevertheless the basic form of the expression (2.30) remains, and is used for practical calculations of the dispersion. The

frequency dependence in wide spectral range typically can be described by two or three so-called Sellmeyer terms, coefficients for which can be found in tables (e.g. [52]). The frequency dependence of $\chi(\omega) = n^2(\omega) - 1$ determines the group velocity $v_g(\omega) = c/[d(\omega n(\omega))/d\omega]$ as well as the dispersion regime. In the normal-dispersion regime, higher-frequency components travel slower than lower-frequency ones ($dv_g/d\omega < 0$), the opposite occurs in the anomalous dispersion regime ($dv_g/d\omega > 0$). For example, bulk fused silica has normal dispersion for the wavelength shorter than 1.27 μm and anomalous dispersion for longer wavelengths.

The expression (2.25) is only the first term in the expansion of $\vec{P}$ in powers of $\vec{E}$, because generally the dependence $\vec{P}(\vec{E})$ is not linear. Rather, it can be represented in the form of series

$$\begin{aligned}\vec{P}_L(t) &= \epsilon_0 \int_0^\infty \hat{\chi}_1(\tau)\vec{E}(t-\tau)d\tau + \\ &\epsilon_0 \iint_0^\infty \hat{\chi}_2(\tau_1,\tau_2)\vec{E}(t-\tau_1)\vec{E}(t-\tau_2)d\tau_1 d\tau_2 + \\ &\epsilon_0 \iiint_0^\infty \hat{\chi}_3(\tau_1,\tau_2,\tau_3)\vec{E}(t-\tau_1)\vec{E}(t-\tau_2)\vec{E}(t-\tau_3)d\tau_1 d\tau_2 d\tau_3 +, \ldots\end{aligned} \tag{2.31}$$

where χ_n is the n-th order susceptibility and we completely exclude nonlocal effects. As in the case of linear susceptibility, transformation into the frequency domain simplifies the expression to

$$\begin{aligned}\vec{P}(\omega) &= \hat{\chi}_1(\omega)\vec{E}(\omega) + \hat{\chi}_2(\omega_1, \omega = \omega_i + \omega_j) : \vec{E}(\omega_i)\vec{E}(\omega_i) + \\ &\hat{\chi}_3(\omega = \omega_i + \omega_j + \omega_k) : \vec{E}(\omega_i)\vec{E}(\omega_i)\vec{E}(\omega_i) + \ldots .\end{aligned} \tag{2.32}$$

Here the susceptibility of n-th order is a tensor of $n+1$'th order, and the : sign expresses corresponding index summation. The relations in the argument of

χ underline the fact that the sum of frequencies of the photons created and destroyed in the nonlinear process must be the same as a consequence of the energy conservation law.

While a full calculation of the nonlinear susceptibilities is possible only by a quantum model, the origins of the nonlinearity can be understood through the model of an anharmonic oscillator. Anharmonicity $a_j x_j^3/3$ is added to the binding potential of j-th group of atoms, so that equation of motion now looks like [53]

$$\frac{d^2\vec{x_j}}{dt^2} + g_j \frac{d\vec{x_j}}{dt} + \omega_j^2 \vec{x_j} + a_j x_j^2 = -\frac{\vec{E}e}{m}. \tag{2.33}$$

To solve it, a perturbative method can be used for not too strong fields. The solution of unperturbed equation (2.28) as given in Eq.(2.30) is substituted in the anharmonical term in (2.33).

The resulting equation can readily be solved. For example, for the component $\chi_2(\omega_1 + \omega_2)$ one gets

$$\begin{aligned} \chi_2(\omega_1, \omega_2) &= \sum_j \frac{-2a_j(e/m)^2}{(\omega_j^2 - \omega_2^2 - i\omega_2 g_j)(\omega_j^2 - \omega_1^2 - i\omega_1 g_j)} \\ &\quad \times \frac{1}{\omega_j^2 - (\omega_1 + \omega_2)^2 - i(\omega_1 + \omega_2) g_j}. \end{aligned} \tag{2.34}$$

In fact, second-order nonlinearity is absent in fibers due to the symmetry $\chi_2 = 0$. However third-order susceptibilities can be derived in a similar way.

This simple classical model illustrates the mechanism of nonlinearity, which is most important in the scope of this work, namely Kerr nonlinearity. In the quantum consideration, it results from the distortion of the electron wavefunctions in the field. There exist several other mechanisms of nonlinearity, such as Raman effect, molecular reorientation, electrostriction, heating, and so on. Among them, only a Raman effect has sufficiently small

response time to play any role in the processes on the femtosecond time scale considered here. In this effect, incident light is scattered by a molecule in a certain initial vibrational state. The molecule is excited to a high-energy electronic state and immediately reemits the photon. However, the final vibrational state of the molecule is different from the initial one, therefore the energy of the photon changes. The stimulated Raman scattering is a third-order nonlinear process which is responsible for about 1/5 of the nonlinear response in the silica. It is known that it introduces a shift of the soliton frequency (see e.g. [54]). However, our numerical simulations show that the Raman effect does not play a significant role in the processes of SC generation in PCFs and hollow fibers, therefore it was not included into considerations.

The nonlinear polarization P_{NL} far off the medium resonance for not too high intensity in a isotropic medium can be treated as a third-order process and is dominated by the Kerr nonlinearity. Sheik-Bahae *et al.* [55] have developed a model for the dispersion of the dominant electronic part of χ_3 for semiconductors and wide-gap optical solids. It gives a universal formula for $\chi_3(\omega_1, \omega_2, \omega_3, \omega_4)$ in quite good agreement with measurements. According to this model for

$$\omega_j \ll \omega_g = \frac{E_g}{\hbar}, \tag{2.35}$$

where $j = 1..4$ and E_g is the bandgap energy, up to the first correction term $\chi_3(\omega, \omega, -\omega, \omega)$ has the form

$$\chi_3 = \chi_3^{(0)} \left(1 + 2.8\frac{\omega^2}{\omega_g^2} + \dots\right) . \tag{2.36}$$

For fused silica it holds that $E_g = 9$ eV and therefore the correction terms do not play a significant role even for the extremely broad spectra considered here. With this estimation the nonlinear polarization is instantaneous, i.e.

$P_{NL}(z,t)$ depends only on the $E(z,t)$ as $\vec{P}_{NL}(z,t) = \epsilon_0 \chi_3^{(0)} E^2(z,t)\vec{E}(z,t)$.

2.1.2 Self-phase modulation

The physical origin of the effect of self-phase modulation is connected with the distortion of the electronic distribution of the media leading to a refractive index change by the electric field $n = n_0 + n_2 I$. It was first observed in 1967 [56] in gases, and later also in solids [57] and optical fibers [58]. The description of this process, which is presented here following Ref. [50], can be done simply in the case when the effects of the linear dispersion can be ignored; this requirement is expressed as $L_D \gg L_{NL}$, where $L_{NL} = 1/(\gamma' A_0^2)$ and $L_D = T_0^2/\beta''$ are characteristic linear and nonlinear lengths, respectively, and $T_0 = \tau_0/1.76$ is related to the initial full-width half-maximum (FWHM) pulse duration τ_0. Then the equation (2.21) for the field can be written as

$$\frac{\partial U}{\partial z} = \frac{i}{L_{NL}} \exp(-2\alpha z)|U|^2 U \tag{2.37}$$

where the variable $U = A/A_0$ is the envelope of the field normalized by its initial value, and α is the field loss. The solution of this equation is [50]

$$U(z,t) = U(0,t)\exp[i\phi_{NL}(z,t)] \tag{2.38}$$

with

$$\phi_{NL}(z,t) = |U(0,t)|^2 \frac{z_{eff}}{L_{NL}}. \tag{2.39}$$

Here z_{eff} is given by

$$z_{eff} = \frac{1}{\alpha}[1 - \exp(-2\alpha z)] \tag{2.40}$$

and is smaller than z thus indicating that the loss limits the SPM. As a result, a time-dependent phase ϕ_{NL} is induced which implies a time-depending

instantaneous frequency shift

$$\delta\omega(t) = -\frac{\partial\phi_{NL}}{\partial t} = -\frac{\partial|U(0,t)|^2}{\partial t}\frac{z_{eff}}{L_{NL}}. \tag{2.41}$$

The chirp is caused by SPM and increases in magnitude with the propagation. This chirp leads to negative $\delta\omega$ on the leading front of the pulse and positive $\delta\omega$ on the trailing edge. Over a large central region, the chirp is almost linear and positive. Consequently, new frequencies are generated on both sides on the input frequency. These SPM-induced components broaden the spectrum over its input width at the input. An estimate of the magnitude of this broadening can be done by maximizing $\delta\omega$ given by the above equation. The result for $U(0,t) = 1/\cosh(t/T_0)$ is

$$\delta\omega_{max} = 0.86\frac{\phi_{max}}{T_0}, \tag{2.42}$$

where ϕ_{max} is the maximum value of the phase shift obtained for $T = 0$, which is given by

$$\phi_{max} = \frac{z_{eff}}{L_{NL}}. \tag{2.43}$$

The resulting spectra have an oscillatory behavior with the number of oscillation approximately equal to ϕ_{max}/π. The reason for this behavior is that the same frequency occurs for two values of t in the expression (2.41) for the frequency shift. Depending on the phase between these components, the interference between them can be constructive or destructive, thus creating the oscillatory behavior.

This consideration is valid only if the group velocity dispersion can be neglected, expressed by the condition $L_D >> L_{NL}$. In the normal dispersion regime, pulse broadening happens faster than in the case when GVD is absent. This is due to the fact that SPM generates new frequency components, which are red-shifted near the leading edge and blue-shifted near

the trailing edge. Red components move faster than the blue components in the normal-dispersion regime. Therefore SPM leads to a larger rate of pulse broadening compared with that expected from GVD alone. The temporal shape for this case becomes characteristically rectangular-like. The reason is that any peak in the temporal shape results in the chirp, and newly created spectral components are pulled apart by the normal dispersion, thus leading to smoothing of the initial peak. Quick elongation of the pulse leads to lowering of the peak intensity and less effective SPM. The ratio of pulse durations with and without GVD, which is reverse of the ratio of intensities for unchanged pulse shape, is given by [59]

$$\frac{\tau}{\tau_0} = \left[1 + \sqrt{2}\phi_{max}\frac{z}{L_D} + \left(1 + \frac{4}{3\sqrt{3}}\phi_{max}^2\right)\frac{z^2}{L_D^2}\right]^{1/2}. \qquad (2.44)$$

Thus for strong normal GVD the spectral broadening becomes less effective due to decreasing peak intensity.

The effects of anomalous GVD are different. For $N = \sqrt{L_D/L_{NL}} \sim 1$ the spectral broadening is stopped by GVD. This happens as soon as the pulse reaches a duration which corresponds to that of a fundamental soliton. For a fundamental soliton, effects of GVD and SPM exactly compensate each other, and no further broadening occurs. For still larger values of N, higher-order solitons can be created, as described in the next subsection.

2.1.3 Optical solitons in fibers

Solitons were first observed as steady waves on a water surface in the 19th century, and since then many systems such as plasma, sound waves, and optical waves have been shown to exhibit solitonic behavior. Optical solitons were first observed in fibers by Mollenauer *et al.* [60].

Let us consider the NSE (2.22), which is the propagation equation for the electromagnetic field in the case when only Kerr–like nonlinearity and second-order dispersion are included:

$$\frac{\partial A}{\partial z} + \frac{i}{2}\beta'' \frac{\partial^2 A}{\partial \eta^2} = i\gamma' |A^2| A. \tag{2.45}$$

It can be transformed to the normalized form by the variable change (see [50] for the summary used here)

$$U = \frac{A}{A_0}, \xi = \frac{z}{L_d}, \tau = \frac{\eta}{T_0} \tag{2.46}$$

where A_0 and $\tau_0 = 1.76T_0$ are the initial pulse amplitude and duration, respectively (here sech-shaped pulses are assumed). Then the equation takes the form

$$i\frac{\partial U}{\partial \xi} = \mathrm{sgn}(\beta'')\frac{1}{2}\frac{\partial^2 U}{\partial \tau^2} - N^2 |U^2| U \tag{2.47}$$

where the parameter N is given by

$$N^2 = \frac{\omega_0 n_2 n A_0^2 T_0^2 \epsilon_0}{2\beta''} = \frac{L_d}{L_{NL}}. \tag{2.48}$$

For $\beta'' < 0$ and $N > 0.5$, solitons can form from the initial pulse, with the number of solitons for the sech-shaped pulse being the integer closest to N. They are a result of the balance between linear dispersion, which introduces negative (anomalous) chirp, and self-phase modulation, which introduces positive chirp.

This equation can be solved by the inverse scattering method [61, 50], which allows to analytically find the solution for (2.47) with any localized initial condition $U(0, \tau)$. The scattering problem associated with Eq. (2.47) written for $u = NU$ is

$$\frac{\partial \nu_1}{\partial \tau} + i\zeta \nu_1 = u\nu_2 \tag{2.49}$$

$$\frac{\partial \nu_2}{\partial \tau} + i\zeta \nu_2 = u\nu_1 \tag{2.50}$$

for the amplitudes $\nu_{1,2}$ of the waves scattered on the potential $u(\xi,\tau)$, and ζ is the eigenvalue. First, initial scattering data in the form of the continuous spectrum $r(\zeta)$ and N poles (bound states) with eigenvalues ζ_j and residues c_j are obtained from the initial field distribution $u(0,\tau)$. Then, the evolution with ξ of the scattering data $r(\zeta);\zeta_j;c_j$ is determined by simple algebraic relations found elsewhere [50, 62]. And finally, the solution $u(\xi,\tau)$ is reconstructed from the scattering data at the point ξ. This last step is especially simple if $r=0$. Then the scattering data in the form of N *constant* eigenvalues ζ_j and the residues c_j correspond to the N solitons, and the field is obtained in the form

$$u(\xi,\tau) = -2\sum_{j=1}^{N} \lambda_j^* \psi_{2j}^* \tag{2.51}$$

where $\lambda_j = \sqrt{c_j}\exp(i\zeta_j\tau + i\zeta_j^2\xi)$ and ψ_{2j} are obtained from the linear set of equations

$$\psi_{1j} + \sum_{k=1}^{n} \frac{\lambda_j\lambda_k^*}{\zeta_j - \zeta_k^*}\psi_{2k}^* = 0 \tag{2.52}$$

$$\psi_{1j} + \sum_{k=1}^{n} \frac{\lambda_j\lambda_k^*}{\zeta_j - \zeta_k^*}\psi_{2k}^* = 0. \tag{2.53}$$

Each term in the sum for u is what is called a *constituent* soliton, a part of radiation determined by the corresponding eigenvalue ζ_j. Generally, N solitons have different $Re(\zeta_j)$ and therefore different central frequencies and different velocities. In the collisions, such solitons preserve their form and amplitude, and experience only a temporal shift. Far from the collision region, each of the constituent solitons is the simplest form of a soliton, which is called a fundamental soliton ($N=1$); the field in this case is described by

$$U(\xi,\tau) = \mathrm{sech}(\tau)\exp(i\xi/2). \tag{2.54}$$

In contrast, if all the central frequencies of the constituent solitons are the same, a *bound higher-order* soliton is formed, which is characterized by periodic (with period $\pi L_D/2$) changes of shape during propagation. The simplest example for a higher-order soliton for $N = 2$ is given by

$$U(\xi,\tau) = \frac{2[\cosh(3\tau) + 3\exp(4i\xi)\cosh(\tau)]\exp(i\xi/2)}{\cosh(4\tau) + 4\cosh(2\tau) + 3\cos(4\xi)}. \tag{2.55}$$

The situation is more complicated if other (higher-order) terms are included in Eq. (2.47) as e.g. in Eq. (2.21). If third-order dispersion (TOD) or the Raman effect are taken into account, the stability of the higher-order soliton is broken. It splits into constituent fundamental solitons with different eigenvalues ζ, which have different frequencies and group velocities. For the propagation of a pulse at the zero-dispersion wavelength, the initial spectrum of the pulse splits into the peak in the anomalous region, which is fundamental soliton, and the peak in the normal region, which constitutes dispersive non-solitonic radiation [63]. The energy contained in both pulses can be approximately of the same magnitude. If the initial frequency is far from the zero-dispersion wavelength, the third-order dispersion can be considered as a perturbation [64]. The perturbed NSE is written in the form

$$i\frac{\partial u}{\partial \xi} - \frac{\partial^2 u}{\partial \tau^2} - 2u|u|^2 = i\epsilon\frac{\partial^3 u}{\partial \tau^3} \tag{2.56}$$

which can always be achieved by the corresponding renormalization of variables. Here $\epsilon = \beta'''/(3\tau_0\beta'')$ is a dimensionless parameter which describes the relative impact of third order dispersion. The fundamental soliton solution (2.54) is modified by the presence of TOD by a small change in the pulse parameters and the emission of a low-level background radiation field. In the first order in ϵ, only the velocity of the soliton reduces by the amount

equal ϵ. All other parameters are unchanged in the first order; to determine them, it is necessary to use the numerical result of Refs. [63, 65]. It is shown there that the frequency at which the soliton is stabilized differs from the input frequency by a value determined from the equation $A\epsilon_c < 0.04$. Here A and ϵ are the dimensionless amplitude and TOD-factor taken at the *final* soliton frequency. If this condition is not initially fulfilled, the soliton emits non-solitonic radiation and shifts away from the zero-dispersion point until the stability is reached. To describe the properties of the non-solitonic radiation, a change of variables is introduced on the basis of the fact that Eq. (2.56) has several conserving quantities, or invariants (for details see [66, 67]). The new independent function $f(\xi, \eta)$ is "associated" with the perturbation $\delta u = u - u_0$ of the fundamental-soliton solution u_0, as given by (2.54) [64]:

$$\delta u = -\frac{\partial^2 f}{\partial \tau^2} + 2\tanh(\tau)\frac{\partial f}{\partial \tau} - \tanh^2(\tau) f + u_0^2 f^*. \tag{2.57}$$

This new field satisfies the linear evolution equation

$$i\frac{\partial f}{\partial \xi} = \frac{\partial^2 f}{\partial \tau^2} + i\epsilon\frac{\partial f}{\partial \tau} - \frac{i\epsilon}{2}\frac{\partial u_0}{\partial \tau} \tag{2.58}$$

and its solutions can be found by Fourier-transforming the previous equation in the form

$$f(\xi,\tau) = -\frac{\epsilon}{4}\int_{-\infty}^{\infty} \frac{\omega \mathrm{sech}\left(\frac{1}{2}\pi\omega\right)}{D(\omega)}\{\exp[i(\omega^2 - \epsilon(\omega^3 - \omega))] - \exp(-i\xi)\}\exp(i\omega\tau)d\omega. \tag{2.59}$$

The dispersion relation $D(\omega) = \omega^2 + 1 - \epsilon(\omega^3 - \omega) = 0$ determines the spectral position of the generated radiation. This condition is equivalent to the phase-matching condition $k_s = k(\omega_r)$, where $k_s = \partial\beta/\partial\omega(\omega_s) - (1/2)n_2 I\omega_s/c$ is the wavenumber of the fundamental soliton at frequency ω_s and ω_r is the frequency of the non-solitonic radiation. The latter condition is also valid if

higher (4th and larger) orders of linear dispersion need to be taken into account, as it is the case for PCF's. In more detail, this condition is considered in Chapter 3, as well as a case of higher-order input soliton.

2.2 Propagation equation in fibers

In a fiber, radiation generally can propagate in several transverse modes. In the absence of birefringence, the energy transfer between the modes can be caused by nonlinear effects. In a single-mode fiber for a power below the critical power of selffocusing $P_{cr} = \lambda_0^2/(\pi n_2)$ the energy transfer to higher transverse modes is weak [27]. In Chapter 5 the this limitation on the maximum intensity will be considered in more detail. The electric field in the frequency domain can be separated [50] into the form:

$$\mathbf{E}(x, y, z, \omega) = \mathbf{F}(x, y, \omega)\tilde{E}(z, \omega), \tag{2.60}$$

where the transverse fundamental mode distribution $\mathbf{F}(x, y, \omega)$ is the solution of the Helmholtz equation

$$\Delta_\perp \mathbf{F} + k(\omega)^2 \mathbf{F} = \beta(\omega)^2 \mathbf{F} \tag{2.61}$$

for a PCF with the eigenvalue $\beta(\omega)$. We substitute (2.60) into (2.5), take account of (2.61), and assume that the dependence of $\vec{F}$ on ω is much weaker than that of $\tilde{E}$. In this way we obtain

$$\begin{aligned} &\vec{F}(x, y, \omega)\frac{\partial^2 \tilde{E}(z, \omega)}{\partial z^2} + \beta^2(\omega)\vec{F}(x, y, \omega)\tilde{E}(z, \omega) = \\ &-\mu_0 \omega^2 F^2(x, y, \omega)\vec{F}(x, y, \omega)P_{NL}(z, \omega) \end{aligned} \tag{2.62}$$

where $P_{NL}(\xi, \eta) = \chi_3 \epsilon_0 \tilde{E}^3(\xi, \eta)$. This equation is multiplied by $\vec{F}$, the integration is taken over the cross-section, and the result is divided by the mode

area

$$S_1(\omega) = \int_S F^2(x, y, \omega) dS. \tag{2.63}$$

The equation obtained in this way is

$$\frac{\partial^2 \tilde{E}(z,\omega)}{\partial z^2} + \left(\beta^2(\omega) + W(\omega)\mu_0\omega^2 B_{NL}(z,\omega)\right)\tilde{E}(z,\omega) = 0, \tag{2.64}$$

where $P_{NL}(z,t) = \chi_3\epsilon_0\tilde{E}^3(z,t)$ and

$$W(\omega) = \frac{\int_S F^4(x,y,\omega)dS}{S_1} \tag{2.65}$$

is a nonlinear reduction factor. We can now follow the same argumentation which allowed to obtain (2.19) from (2.5). With the introduction of the moving time coordinates $\xi = z, \eta = t - zn_g/c$, the longitudinal distribution $\tilde{E}(\xi,\omega)$ satisfies the equation

$$\frac{\partial\tilde{E}(\xi,\omega)}{\partial\xi} = i\frac{[n(\omega)-n_g]\omega}{c}\tilde{E}(\xi,\omega) + i\mu_0 c\frac{\omega}{2n(\omega)}W(\omega)P_{NL}(\xi,\omega). \tag{2.66}$$

Here $P_{NL}(\xi,\eta) = \chi_3\epsilon_0\tilde{E}^3(\xi,\eta)$. This equation can be used to model the propagation of ultrashort light pulses in fibers, and has the same advantages as the FME equation (2.19). The additional requirement that power be much less than the power of selffocusing makes it possible to reduce the dimension of the problem, i.e. the unknown function $\tilde{E}$ depends on only one spatial coordinate in (2.66).

2.2.1 Waveguiding model for a step-index fiber

The description of a step-index fiber is done in a standard way found elsewhere [68, 69]. Let us consider a step-index fiber, which consists of a core with radius a and refractive index n_0 surrounded by unlimited cladding with refractive index n_1, $n_0 > n_1$. The problem is to determine the wavenumber

β for a mode with frequency ω. The temporal and longitudinal dependence of the electric and magnetic fields of the mode is given by $\exp(i\omega t - i\beta z)$. The Helmholz equation for each of these fields is given by [68, 69]

$$\frac{\partial^2}{\partial\rho^2} + \frac{1}{\rho}\frac{\partial}{\partial\rho} + \frac{1}{\rho^2}\frac{\partial^2}{\partial\phi^2} + n_{0,1}^2 k_0^2 - \beta^2 = 0. \tag{2.67}$$

Here $k_0 = \omega c$, ϕ is the azimutal coordinate of a cylindrical coordinate system with the axis directed along the axis of the fiber; the dependence of the field in this direction is fixed for each mode and is given by $\exp(il\phi)$ where l is the azimuthal order of the mode. This dependence follows from the fact that any field should be a periodic function of ϕ. It is useful to introduce denotations $V = \sqrt{n_0^2 - n_1^2}ak_0$, $u = a\sqrt{n_0^2 k_0^2 - \beta^2}$, and $v = a\sqrt{\beta^2 - n_1^2 k_0^2}$, where $k_0 = \omega/c$. The Helmholtz equation then transforms to a differential equation in the ρ direction

$$\frac{d^2}{d\rho^2} + \frac{1}{\rho}\frac{d}{d\rho} + \left(a^2u^2 - \frac{l^2}{\rho^2}\right) = 0 \tag{2.68}$$

in the core ($\rho < a$) and

$$\frac{d^2}{d\rho^2} + \frac{1}{\rho}\frac{d}{d\rho} + \left(-a^2v^2 - \frac{l^2}{\rho^2}\right) = 0 \tag{2.69}$$

in the cladding ($\rho > a$). The solutions are given by Bessel functions. If we account for boundary conditions (all fields should be zero at infinitely large radius and have finite values at $\rho = 0$), then the fields inside (outside) the

core are given by (modified) Bessel functions of first (second) type:

$$E_{z1} = A_E J_l(u\rho/a)\cos l\phi \tag{2.70}$$

$$H_{z1} = A_H J_l(u\rho/a)\sin l\phi \tag{2.71}$$

$$E_{\rho 1} = -j\frac{a}{u}[\beta A_E J_l'(u\rho/a) + \omega\mu_0\frac{la}{u\rho}A_H J_l(u\rho/a)]\cos l\phi \tag{2.72}$$

$$H_{\rho 1} = -j\frac{a}{u}[\beta A_H J_l'(u\rho/a) + \omega\epsilon_0 n_0^2\frac{la}{u\rho}A_E J_l(u\rho/a)]\cos l\phi \tag{2.73}$$

$$E_{\phi 1} = j\frac{a}{u}[\frac{l\beta a}{u\rho}A_E J_l(u\rho/a) + \omega\mu_0 A_H J_l'(u\rho/a)]\sin l\phi \tag{2.74}$$

$$H_{\phi 1} = -j\frac{a}{u}[\frac{l\beta a}{u\rho}A_H J_l(u\rho/a) + \omega n_0^2\epsilon_0 A_H J_l'(u\rho/a)]\sin l\phi \tag{2.75}$$

in the core and

$$E_{z2} = D_E K_l(v\rho/a)\cos l\phi \tag{2.76}$$

$$H_{z2} = D_H K_l(v\rho/a)\sin l\phi \tag{2.77}$$

$$E_{\rho 2} = -j\frac{a}{v}[\beta D_E K_l'(v\rho/a) + \omega\mu_0\frac{la}{v\rho}D_H K_l(v\rho/a)]\cos l\phi \tag{2.78}$$

$$H_{\rho 2} = -j\frac{a}{v}[\beta D_H K_l'(v\rho/a) + \omega\epsilon_0 n_1^2\frac{la}{v\rho}D_E K_l(v\rho/a)]\cos l\phi \tag{2.79}$$

$$E_{\phi 2} = j\frac{a}{v}[\frac{l\beta a}{v\rho}D_E K_l(v\rho/a) + \omega\mu_0 D_H K_l'(v\rho/a)]\sin l\phi \tag{2.80}$$

$$H_{\phi 2} = -j\frac{a}{v}[\frac{l\beta a}{v\rho}D_H J_l(v\rho/a) + \omega n_0^2\epsilon_0 D_H K_l'(v\rho/a)]\sin l\phi \tag{2.81}$$

in the cladding. The constants A and D have to be chosen so that the fields satisfy boundary conditions at $\rho = a$. In the general case of large refractive index difference, the boundary condition yields a system of homogeneous linear equations for A and D. Solution of this system exists if the determinant is equal to zero, which yields the following dispersion relation for the step-index fibers in the general case:

$$l^2\frac{\beta^2}{k_0^2}\left(\frac{1}{u^2}+\frac{1}{v^2}\right)^2 = (Y_1 n_0^2 + X_1 n_1^2)(Y_1 + X_1) \tag{2.82}$$

where $X_l = K_l'(v)/(vK_l(v))$ and $Y_1 = J_m'(u)/(uJ_m(u))$. This equation is to be solved together with $u^2+v^2 = V^2$ to obtain unknown variables u and v and thus β as function of ω. The detailed analysis of this equation, which is out of the scope of this work, shows that there always exists one solution, which corresponds to the fundamental mode EH_{11}. For V larger than the threshold value of approximately 2.405, other modes can be excited. In this work, only radiation in the fundamental mode is considered. The simplification of the dispersion equation is possible for weakly guiding fibers with $n_1 \approx n_0$. In this case for the fundamental mode

$$\frac{uJ_1(u)}{J_0(u)} = \frac{vK_1(v)}{K_0(v)}. \tag{2.83}$$

However, for all problems considered here the full equation (2.82) was used because of a large step between the refractive indexes of core and cladding in the photonic and tapered fibers.

2.2.2 Effective cladding model for PCF's

For the tapered and photonic fibers, no closed analytical expression for the transverse mode distribution exists. There are two common approaches to the calculation of the dispersive properties of the PCF's: the full vectorial model [70] and the approximate effective-cladding model. While for photonic band gap guiding only the full model can give correct results, for the guiding by the full internal reflection (as in the standard fibers) the effective-cladding model [2] gives satisfactory results which coincide with the experimental ones. It was recently shown that in this case the periodic structure of the PCF does not play a decisive role in the waveguiding properties [71]. The abovementioned method to describe the effective cladding is used in this work, as

shown in this subsection. To study pulse propagation in PCF's besides the evolution equation presented in Section 2.2 we need a model for the PCF waveguide contribution to dispersion, which is calculated by the following two-step procedure illustrated in Fig. 2.2. First, an infinite photonic crystal

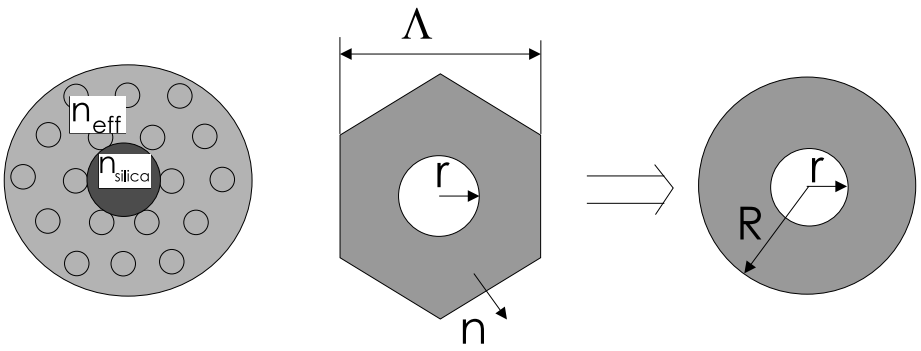

Figure 2.2: Effective-cladding model for calculation of dispersion in PCF's and elementary cell transformation. The hexagonal cell of the effective cladding with refractive index n_{eff} with a continuity boundary condition is transformed into circular cell.

fiber without central defect (core) is considered. The fundamental space-filling mode in such a system can be analyzed in the scalar approximation, i.e. the transverse dependence of all components of both electric and magnetic fields are given by the same function $F(\omega, x, y)$. This function satisfies the Helmholtz equation. Besides that, the fundamental mode has the same periodical properties as the photonic crystal. We split the photonic crystal into the elementary hexagonal cells so that the air holes are in the center of the cells. From the periodicity of $F(\omega, x, y)$ and from the condition that the derivative of F is continuous, it follows that the derivative $\partial F/\partial \vec{n}$ vanishes at the cell boundary, where $\vec{n}$ is the vector normal to the boundary. To further simplify the calculations, we consider a circular cell instead of the hexagonal

one. The radius of the inner air cylinder in the circular cell equals $d = 2r$, the outer radius is defined by the air fraction in the original crystal as

$$R = \Lambda\sqrt{\sqrt{3}/(2\pi)}. \tag{2.84}$$

Now we consider the function $F(\omega, x, y)$ in the polar coordinates as $F(\omega, \rho, \varphi)$. The condition

$$\frac{\partial F}{\partial \vec{n}} = 0 \tag{2.85}$$

transforms to

$$\left.\frac{\partial F}{\partial \rho}\right|_R = 0, \tag{2.86}$$

and the continuity conditions on the inner air-silica interface have to be satisfied as well. In the inner $(0 < \rho < r)$ area, it holds that

$$\beta^2(\omega) - n_{Air}^2(\omega)\omega^2/c^2 = \kappa^2(\omega) > 0 \tag{2.87}$$

and therefore $F \sim I_0(\kappa(\omega)\rho)$, where I is the modified Bessel functions of first type. In the outer area $(r < \rho < R)$ we write

$$\beta^2(\omega) - n_{Silica}^2(\omega)\omega^2/c^2 = -\gamma^2(\omega) < 0 \tag{2.88}$$

and F is equal to the linear combination of J_0 and Bessel function of second order N_0 with coefficients chosen so that the boundary condition at R is satisfied:

$$F(\omega, \rho) \sim J_0(\gamma(\omega)\rho) - N_0(\gamma(\omega)\rho)\frac{J_1(\gamma(\omega)R)}{N_1(\gamma(\omega)R)}. \tag{2.89}$$

Substituting $F(\omega, \rho)$ into the boundary conditions we obtain the dispersion equation

$$\kappa(\omega)\frac{I_1(\kappa(\omega)r)}{I_0(\kappa(\omega)r)}\left[J_0(\gamma(\omega)r) - N_0(\gamma(\omega)r)\frac{J_1(\gamma(\omega)R)}{N_1(\gamma(\omega)R)}\right] =$$

$$-\gamma(\omega)\left[J_1(\gamma(\omega)r) - N_1(\gamma(\omega)r)\frac{J_1(\gamma(\omega)R)}{N_1(\gamma(\omega)R)}\right]. \tag{2.90}$$

This equation is solved together with

$$\kappa^2(\omega) + \gamma^2(\omega) = [n^2_{Silica}(\omega) - n^2_{Air}(\omega)]\omega^2/c^2 \tag{2.91}$$

to find subsequently $\kappa(\omega)$, $\beta(\omega) = (\kappa^2(\omega) + n^2_{Air}(\omega)\omega^2/c^2)^{1/2}$ and the effective refractive index for the fundamental space-filling mode $n_{eff}(\omega) = \beta(\omega)c/\omega$.

Then we consider the omitted hole as a core of a step-index fiber with diameter $2r = 2\Lambda - d$, where Λ is the center-to-center distance between the holes (pitch) and d is the hole diameter, and the surrounding photonic crystal as homogeneous cladding with refractive index $n_{eff}(\omega)$. Note that for certain PCF's the air holes are very large and therefore the central core is supported by the very thin bridges of silica which can be neglected in the calculation of $\beta(\omega)$ and such a fiber can be described as an isolated strand of silica surrounded by air. The dispersion of tapered fiber, which is a μm-scale silica core surrounded by air, can be described in the same way.

2.2.3 Dispersion in hollow fibers

For hollow fibers, the transverse structure and dispersive properties of the modes can be found analytically, as it was done in Ref. [72] and reproduced here. These properties were derived for the conditions $\lambda/a \ll 1$ and $\sqrt{\nu^2 - 1} \gg \lambda/a$. Here a is the radius of the hollow fiber, ν is the ratio of the refractive indices of the hollow fiber walls and the gas filling. These requirements are satisfied with high accuracy for the typical values $\lambda = 0.8$ μm, $a = 100$ μm, ν=1.45 (for fused silica cladding), which allows simplification of general equations. The expressions for the fields are derived from the Helmoltz equation and from the continuity boundary conditions $E_\phi(a-0) = E_\phi(a+0)$, $E_z(a-0) = E_z(a+0)$, $D_z(a-0) = D_z(a+0)$ set

at $\rho = a$. There exist three types of modes in such a system (as well as in a step-index fiber): transverse electric, or TE_{0m} ($E_z = 0$), transverse magnetic, or TM_{0m} ($H_z = 0$), and hybrid EH_{lm} (both electric and magnetic field have nonzero z component). The index l characterizes the azimuthal dependence of the mode $\exp(il\phi)$, m is the order of the mode. The distribution of fields in the cross-section plane for the case $\lambda/a \ll 1$ is

$$E_\phi = -\sqrt{\frac{\mu_0}{\epsilon_0}} H_r = J_1\left(u_{0m}\frac{\rho}{a}\right) \tag{2.92}$$

for TE_{0m} modes,

$$E_r = \sqrt{\frac{\mu_0}{\epsilon_0}} H_\phi = J_1\left(u_{0m}\frac{\rho}{a}\right) \tag{2.93}$$

for TM_{0m} modes, and

$$E_\phi = -\sqrt{\frac{\mu_0}{\epsilon_0}} H_r = J_{n-1}\left(U_{0m}\frac{\rho}{a}\right)\cos n\phi \tag{2.94}$$

$$E_r = \sqrt{\frac{\mu_0}{\epsilon_0}} H_\phi = J_{n-1}\left({}_{0m}\frac{\rho}{a}\right)\sin n\phi \tag{2.95}$$

for hybrid EH_{lm} modes. Here U_{lm} is the m'th root of the equation $J_{l-1}(U_{lm}) = 0$. The dispersion relation is given by

$$J_{n-1}(\sqrt{k_0^2 - \beta^2}a) = i\Lambda_x \frac{\sqrt{k_0^2 - \beta^2}a}{k_0} J_n(\sqrt{k_0^2 - \beta^2}a) \tag{2.96}$$

and for low-order modes, β can be explicitly expressed:

$$\beta_{lm} = \frac{\omega n(\omega)}{c}\left(1 - \frac{1}{2\gamma_g^2}\right) \tag{2.97}$$

with the field loss determined by

$$\alpha_{lm} = \frac{\Re(\Lambda_x)}{R_g^2 R}. \tag{2.98}$$

Here $n(\omega)$ is the refractive index of the fiber filling, and the parameters R_g and Λ_x are introduced by

$$R_g = \frac{2\pi R}{U_{lm}\lambda} \tag{2.99}$$

and

$$\Lambda_x = \begin{cases} \frac{1}{\sqrt{\nu^2-1}} & \text{for } \mathrm{TE}_{0\mathrm{m}} \text{ modes} \\ \frac{\nu^2}{\sqrt{\nu^2-1}} & \text{for } \mathrm{TM}_{0\mathrm{m}} \text{ modes} \\ \frac{\nu^2+1}{2\sqrt{\nu^2-1}} & \text{for } \mathrm{EH}_{\mathrm{lm}} \text{ modes} \end{cases} . \tag{2.100}$$

With propagation, only the mode with lowest loss will remain in the waveguide. In this case it is the EH_{11} mode [73], for which the transverse distribution of intensity is given by $J_0(a_1\rho/a)$. Here r is the transverse coordinate and a_1 is the first zero of the Bessel function J_1. The contribution of the waveguide to the dispersion in this case is given by [73]

$$\beta(\omega) = k(\omega) - \frac{1}{2}\left(\frac{2.405c}{\omega a}\right)^2 \left[\frac{\omega}{c} - i\frac{1+\nu^2}{a\sqrt{\nu^2-1}}\right]. \tag{2.101}$$

The hollow waveguide is not truly a guiding system in the sense that it possess no lossless modes. Therefore the loss, which is inversely proportional to a^3, is introduced. Our calculations show that the values $W = 0.567$ and $S_1 = 0.269\pi a^2$ do not depend on frequency in the case of the hollow fibers.

2.2.4 Nonlinear term for propagation in fibers

This procedure allows us to determine the dispersion of PCF or tapered fibers as determined by the function $\beta(\omega)$. The dependence of the mode area S_1 and frequency can also be determined with this model. A typical case is presented in Fig. 2.3. Although there exits a slight variation of W in the infrared, we neglect this effect because dominant part radiation has shorter wavelength in all spectra considered here. A similar physical picture can be observed for other fibers considered in this work.

In the literature, for the case of the NSE the definition of envelope which differs from (2.1) is often used. The envelope $A_*(\xi,\eta) = A(\xi,\eta)\sqrt{\epsilon_0 ncS_1/2}$

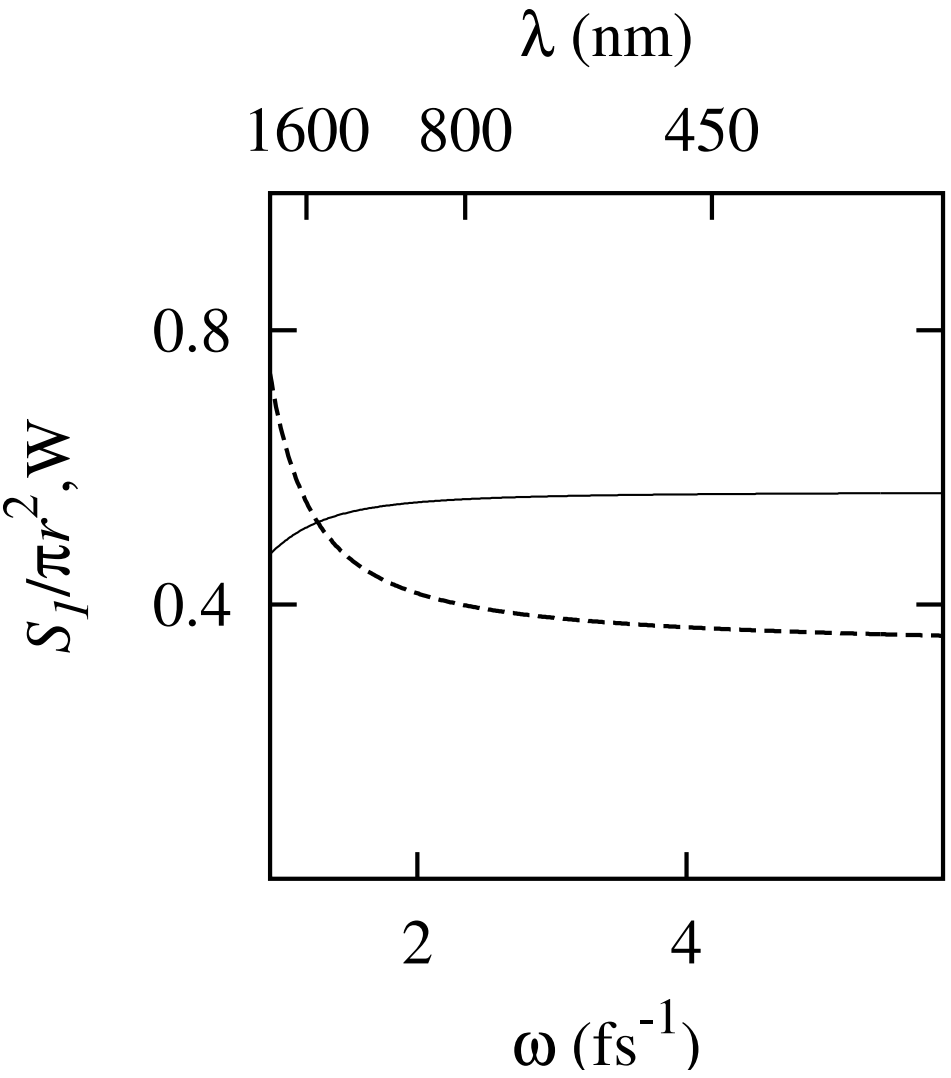

Figure 2.3: Nonlinear reduction factor W (solid) and mode area S_1 (dotted) as functions of frequency for PCF with Λ=1.5 μm and d=1.3 μm.

is normalized so that A_*^2 gives the power of the pulse. In this normalization, the NSE (2.22) reads as

$$\frac{\partial \vec{A}_*}{\partial z} + \frac{i}{2}\beta'' \frac{\partial^2 \vec{A}_*}{\partial \eta^2} = i\gamma \left(|A_*^2| \vec{A}_* \right) \ . \tag{2.102}$$

where $\gamma = \omega_0 n_2/(cA_{eff})$ with

$$A_{eff}(\omega) = \frac{\left(\int_S F^2(x,y,\omega)dS\right)^2}{\int_S F^4(x,y,\omega)dS} = \frac{S_1(\omega)}{W(\omega)}. \tag{2.103}$$

The value A_{eff} is usually called effective mode area. This description gives an equivalent way to express the nonlinear term, but the quantity S_1 is useful because it relates power and peak intensity.

2.3 Numerical procedure

For the numerical simulation of Eq. (2.66), the split-step Fourier method was used. The right-hand side of this equation can be separated into linear and nonlinear parts. We then define operators $\hat{G}_L(dz)$ and $\hat{G}_{NL}(dz)$ for linear and nonlinear dz-steps, each of which consist of a propagating field $\tilde{E}(\xi,\omega)$ over dz by linear and nonlinear right-hand terms in (2.66), respectively. It can be shown [50] that using a certain sequence of such operators one can build a second-order (in dz) method for the simulation of the field propagation. For a spatial grid with N+1 points this sequence reads as follows:

$$\hat{G}_L(dz/2)[\hat{G}_{NL}(dz)\hat{G}_L(dz)]^{N-1}\hat{G}_N L(dz)\hat{G}_L(dz/2). \tag{2.104}$$

It is possible to construct fourth- and higher-order methods in this way [74], which however were not implemented in this work, because they significantly complicate the program without guaranteeing faster calculations.

Note that linear and nonlinear steps in this method are performed in the different spaces: in the frequency and time space, respectively. For the linear step, the corresponding equation is written in the frequency space as

$$\frac{\partial\tilde{E}(\xi,\omega)}{\partial\xi} = i\frac{[n(\omega)-1]\omega}{c}\tilde{E}(\xi,\omega) \tag{2.105}$$

and can be solved exactly:

$$\hat{G}_L(dz) = \exp\left(i\frac{[\Re n(\omega) - 1]\omega dz}{c}\right)\exp(\alpha(\omega)dz)\tilde{E}(\xi,\omega), \tag{2.106}$$

where $\alpha(\omega)$ is the loss. The nonlinear step is expressed by the following equation in the time domain:

$$\frac{\partial\tilde{E}(\xi,t)}{\partial\xi} = \mu_0\epsilon_0 c\chi_3\frac{W}{2n}\frac{\partial}{\partial t}\tilde{E}^3(\xi,t), \tag{2.107}$$

and we assume $W(\omega)/n(\omega) \sim$ const. To improve the accuracy of the method it is necessary to make the nonlinear step by a method with higher order than the split-step fourier method [75], therefore in this work a fourth-order Runge-Kutta method was used for solving Eq.(2.107):

$$\Delta E_1(t) = C\frac{\partial\tilde{E}^3(z,t)}{\partial t} \tag{2.108}$$

$$\Delta E_2(t) = C\frac{\partial(\tilde{E}(z,t) + \Delta E_1(t)/2)^3}{\partial t} \tag{2.109}$$

$$\Delta E_3(t) = C\frac{\partial(\tilde{E}(z,t) + \Delta E_2(t)/2)^3}{\partial t} \tag{2.110}$$

$$\Delta E_4(t) = C\frac{\partial(\tilde{E}(z,t) + \Delta E_3(t))^3}{\partial t} \tag{2.111}$$

$$\tilde{E}(z+dz,t) = \tilde{E}(z,t) + \frac{1}{6}[\Delta E_1(t) + 2\Delta E_1(t) + 2\Delta E_1(t) + \Delta E_1(t)] \tag{2.112}$$

where $C = dzW\chi_3/(2cn)$ and $\Delta E_{1,2,3,4}(t)$ are the approximations of the Runge-Kutta method.

The sequence (2.104) implies that the Fourier transform has to be performed between the linear and nonlinear steps. However this does not significantly increase the calculation time due to the application of a fast Fourier transform algorithm. A homogeneous rectangular grid was used for the numerical simulations. The time step dt was chosen to be 0.0276 fs to accu-

rately resolve the carrier oscillations even for the high-frequencies components which have a period around 1 fs. The number of time points was 2×10^5 in most calculations, which yields the time window T_w of 5.52 ps. The corresponding resolution in the frequency domain is 0.0227 fs^{-1}. The spatial step dz was chosen around 1 μm. The time differential operator in (2.112) is implemented by the central second-order difference $\partial\tilde{E}^3(z,t)/\partial t = (\tilde{E}^3(z,t+dt) - \tilde{E}^3(z,t-dt))/(2dt)$. The numerical error introduced by this algorithm was estimated by repeating the calculations with the halved spatial step; the comparison of the result shows that the error does not exceed 1%.

The initial condition $E(0,t) = E_0\cos(\omega_0 t)/\cosh(1.76t/\tau_{FWHM})$ is taken at $\xi = 0$. The question of nonreflecting boundary conditions, which have to be imposed for $t = -T_w/2$ and $t = +T_w/2$, is important in many numerical methods involving modeling of propagation [76, 77]. Without boundary conditions, the radiation would reflect from the planes $t = \pm T_w/2$ and thus create numerical artifacts. In the case considered here, instead of using nonreflecting boundary conditions for the extreme points in the temporal grid, the grid was looped to achieve a stable and simple way to account for waves which move too slowly or too quickly with respect to the main radiation and go beyond the time window. Such waves will simply appear on the other side of the domain. Looping is done automatically in frequency-space steps, and the corresponding modification of the central difference allows looping also for the nonlinear step. Of course one has to ensure that waves do not overlap after making the round-trip over the domain. This method has the additional advantage that it does not require preliminary knowledge of the velocities of the waves.

The numerical simulations were performed on a workstations with an Alpha CPU at 667 MHz. The typical computation time was around 24 hours.